IJE TRANSACTIONS A: Basics Vol. 36 No. 07, (July 2023) 1287-1299

International Journal of Engineering

Journal Homepage: www.ije.ir

Experimental and Numerical Investigation of the Impact of Basalt Fibers and Tie Spacing on Short Concrete Column Behavior

Q. A. Hassan[a], A. M. Jabbar*[b], D. H. Mohammed[a]

[a] *Civil Engineering Department, University of Technology, Baghdad, Iraq*
[b] *Civil Engineering Department, College of Engineering, Wasit University, Iraq*

PAPER INFO

Paper history:
Received 18 March 2023
Received in revised form 21 April 2023
Accepted 27 April 2023

Keywords:
Basalt Fiber
Short Column
Cracking Load
Loading Capacity
Tie Spacing
Reinforcement Ratio

ABSTRACT

This paper demonstrates the effect of adding basalt fibers into a concrete matrix and altering tie spacing on the behavior of short concrete columns since short columns are more robust than long ones and are primarily used in structures. Also, the impact of changing the reinforcement ratio on column behavior is numerically discovered. Three volume fractions of basalt fiber and three-tie spacing are adopted. The results illustrate that no-fiber columns sustain more than 50 % of the failure load before cracking, while this percentage raised to 75 % upon adding basalt fiber to concrete. 0.3 % of basalt fiber increases the compressive strength, cracking and ultimate column loads better than 0.6 %. Likewise, the impact of basalt fiber on the crack load is more pronounced than on the maximum load of the column. Basalt fiber columns exhibit lower longitudinal displacement than no-fiber ones at the cracking state. The shortening increases with increasing tie spacing, whereas decreasing tie spacing barely increases the ultimate load of the column. The numerical analysis provides close results to the experimental ones and shows that increasing the reinforcement ratio raises the column's load capacity. For the same tie spacing, increasing the reinforcement ratio raises the loading capacity of columns, and the longitudinal displacement barely increases upon increasing spacing. Generally, basalt fibers delay cracking and improve the column loading capacity.

***doi**: 10.5829/ije.2023.36.07a.10*

NOMENCLATURE

BF	Basalt fiber	Pcr/Pcro	Crack load of fiber column to crack load of analogous no fiber column ratio
BFRC	Basalt fiber reinforced concrete	Pcr/Pu	Cracking to maximum load ratio
COV	Coefficient of Variation	Pu	Maximum load, kN
f'c	Compressive strength, MPa	S	Tie-spacing, mm
FE	Finite element	SD	Standard Deviation
LVDT	Linear Variable Differential Transformer	Δcr	longitudinal displacement at cracking load, mm
Pcr	Cracking load, kN	Δu	longitudinal displacement at maximum load, mm

1. INTRODUCTION

Basalt fiber is a new natural fiber extracted from frozen lava of volcanic rocks gathered on the surface of the earth's crust [1-4]. Basalt fiber has high stability and insulating features [5, 6]. The main property that makes basalt fiber attractive for the use in concrete is its high ability to absorb strain energy upon increasing the load and enhancing the ductility [7], besides its contribution to reduce the drying shrinkage, which improves the impermeability of concrete and increasing the strength and load capacity of structural elements. Many studies investigated the impact of adding basalt fibers on the mechanical properties of concrete. Different percentages as volume fractions or as a percent of cement content were added to the concrete matrix to show their effect and to decide the best content. Each researcher selected the optimal ratio according to the added percentages in the

*Corresponding Author Email: adilmahdi@uowasit.edu.iq
(A. M. Jabbar)

Please cite this article as: Q. A. Hassan, A. M. Jabbar, D. H. Mohammed, Experimental and Numerical Investigation of the Impact of Basalt Fibers and Tie Spacing on Short Concrete Column Behavior, ***International Journal of Engineering, Transactions A: Basics***, Vol. 36, No. 07, (2023), 1287-1299

experiments where these percentages differ from one to another. Qin et al. [8] found that increasing basalt fiber content raised splitting tensile strength, and 1.25 % awarded the highest increment. Kirthika and Singh [9] decided that 0.75 % gave more increment in tensile strength, while 0.5 % accorded the best compressive strength. Ramesh and Eswari [10] found that 1.5 % basalt fiber content awarded the highest tensile strength, while Jia et al. [11] found that 0.2 % basalt fiber assigned the highest tensile strength among three percentages: 0.1, 0.2, and 0.3 %.

For compressive strength: several researchers suggested that basalt fibers have no significant effect. The researchers attributed that to reducing workability upon adding basalt fibers because of the large surface area of the microfiber and suggested using a superplasticizer to improve the concrete workability[1]. Sun et al. [12] found that the 6 mm length fiber and 0.2 % volume fraction awarded the best effect on concrete specimens. Jia et al. [11] concluded that the compressive strength was slightly enhanced upon adding basalt fiber up to 0.2 %, while at 0.3 % basalt fiber, the compressive strength decreased. Li et al. [13] found that the compressive strength slightly declined with the addition of basalt fibers as compared to plain concrete. However, the failure mode was changed from brittle to ductile in compression. Dilbas and Cakir [14] found that the 0.25 % basalt fiber awarded the best increment in compressive strength, while 1.0 % content gave the best result for tensile strength.

Ayub et al. [6] investigated the impact of 1.0 %, 2.0 %, and 3.0 % basalt fiber on the mechanical properties of high-performance concrete (HPC). The results showed that adding basalt fiber at 1.0 % and 2.0 % slightly increased compressive and tensile strength, while 3.0 % basalt fiber content decreased compressive strength by 9.45 % compared to HPC without fiber.

Ghanbari et al. [15] investigated the addition of basalt fibers to ultra-high-performance concrete (UHPC). The results showed that 0.5 %, 1.0, and 1.5 % basalt fiber raised compressive strength by 44 %, 51 %, and 41 %, respectively. High et al. [16] clarified that 1.78 kg/m^3 basalt fibers raised the compressive strength of normal concrete at 3 days by 5.48 %, at 7 days by 14.12 %, and at 28 days by 5.63 %. Krassowska and Kosior [17] showed the incorporation of 2.5 kg/m^3 and 5.0 kg/m^3 basalt fiber into normal concrete increased the compressive strength by 4.75 % and 0.98 %, respectively. Hirde and Shelar [18] clarified that the maximum increment in compressive strength was at 3 % content, while 4 % awarded the highest increment in splitting tensile strength by 33.6 %. Iyer et al. [19] showed that 18 kg/m^3 was the best content to improve compressive and flexural strengths. Incorporating basalt fibers into concrete reduced drying shrinkage and contributed to minimizing the voids in size and quantity [20]. On the other hand, incorporating basalt fibers with the concrete matrix can enhance the absorbed energy and ductility [21]. Also, the numerous basalt filaments for any volume fraction and their orientation in different directions contribute to disrupting cracks in the concrete and impeding their progress, which highly improves the strength [15, 21]. Therefore, basalt fibers act to confine concrete internally.

Generally, it appears that adding basalt fibers to normal, high, and ultra-high-strength concrete can enhance their mechanical properties. Increasing compressive strength can affect the loading capacity of the compressive members, such as columns in buildings and infrastructures.

Columns are the prime compression members [22]. The loading capacity of short columns depends on the concrete cross-section resistance and the stresses carried by the longitudinal rebar [23]. However, steel ties are always used as transverse reinforcement to prevent the buckling of individual longitudinal bars and to hold them in place before and during concrete pouring [23]. Therefore, ACI 318-Code [7], Eurocode 2 [24], and other codes regarded only the concrete cross-section and longitudinal rebars and excluded transverse steel ties in determining the nominal strength of columns, despite the ties having a significant action in confining the concrete. The confining role of the ties for concrete can increase the compressive strength of the concrete and thus increase the bearing capacity of the column [25, 26]. Mokhtar et al. [27] investigated the influence of tie spacing on the behavior of short columns. They found that decreasing tie-spacing increases bearing capacity. Also, the longitudinal displacement increased with decreasing the tie spacing due to raising the confinement effect on concrete. Hoshitha et al. [20] also studied the effect of tie spacing on short columns. Test results showed increasing cracking and ultimate loads with decreasing spacing between ties. That was due to the enhancement of lateral confinement for the concrete core. Naji et al. [28] investigated on Columns Reinforced with Steel Fibers Mokhtar et al. [27] studied the influence of distribution ties on short-column loading capacity. The results showed that more stress occurred near the fixed end of the column. Nemati- Aghamaleki et al. [29] studied on compressive behavior of concrete-filled double-skin circular tubes with active confinement.

According to the action of basalt fibers in providing internal confinement and ties in providing external confinement for concrete in columns, the idea of this study arose. Therefore, this study aims to demonstrate the effect of tie spacing and the addition of basalt fibers to the concrete matrix on the behavior of short column and their loading capacity. Three tie-spacing and three basalt fiber volume fractions are assumed. Three columns with

[1] www.galencomposite.ru

variable tie spacing per mix are cast to arrive at nine columns. Furthermore, three bar diameters are adopted as additional parameters, which are numerically investigated via Abaqus software to show their impact on the short-column behavior, as illustrated in Figure 1.

2. EXPERIMENTAL INVESTIGATION

2. 1. Test Specimens Nine identical circular section short columns were prepared for testing. The column had a diameter of 150 mm and a length of 750 mm. The longitudinal rebars were equal for all columns using 4 bars of 8 mm diameter to give a reinforcement ratio of 1.13 %. The ties were 5.5 mm diameter bars. The concrete cover was 20 mm. The tie spacing was 80 mm, 120 mm, and 180 mm, as shown in Figure 2. Another parameter adopted was the addition of basalt fibers to the concrete matrix to clarify their effects. According to the results obtained from the literature, the lower percentages of basalt fibers have a better effect on concrete strength. Therefore, three-volume fractions were assumed; 0.0, 0.3 %, and 0.6 %.

2. 2. Material Properties and Mix Proportion The mechanical properties of steel rebars used in the columns are listed in Table 1. Tensile testing of rebars are performed according to ASTM A370 [30] and EN 10002 [31].

An identical mixture was used for all columns. The change was in chopped basalt fiber volume fraction and high-range water reducer admixture (HRWRA) dosages. Ordinary Portland cement (ASTM Type I) conforms to ASTM C150-16 [30], a fine natural aggregate with a fineness modulus of 2.75 and compacted density of 1656 kg/m^3, was used in the mixtures. Coarse aggregate was natural crushed gravel with a maximum size of 14 mm and compacted density of 1527 kg/m^3. Fine and coarse aggregate conform to Iraqi Specifications (IS No. 45/1984) [32]. Three volume fractions of basalt fiber were added to a similar concrete mixture, 0.0 %, 0.3 %, and 0.6 %. Therefore, three mixes were prepared to cast nine columns.

Chopped basalt fibers as short filaments collected in slices of 12 mm long and (16-18) μm diameter were utilized, as shown in Figure 3. Basalt fiber has a modulus of elasticity of (85-90) GPa, a density of 2800 kg/m^3, and 3.2 % elongation at breaking [3]. Basalt fiber

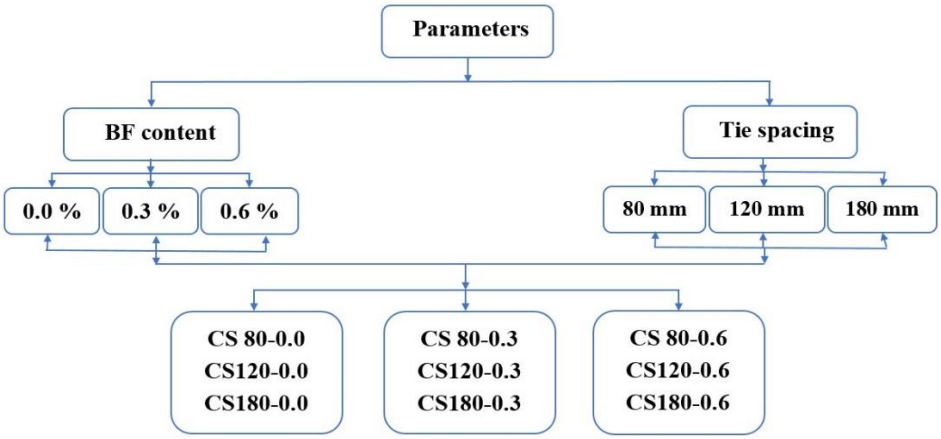

Figure 1. Parameters and experiments scheme

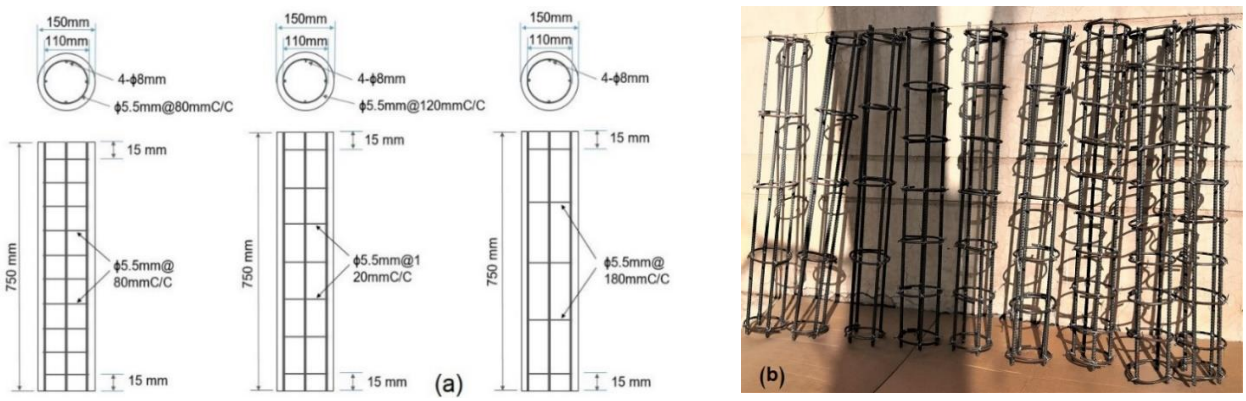

Figure 2. (a) Details of columns showing the spacing between the ties (b) Rebar configuration

TABLE 1. Mechanical properties of steel rebars used in the experiments

Nominal diameter mm	Actual diameter, mm	Rebar area, mm^2	Yield stress, fy, MPa	SD	Ultimate strength, fu, MPa	SD	Modulus of elasticity, Es, GPa	Maximum elongation, %	SD
8.0	7.954	49.69	563	3.64	624	4.06	200	7.678	0.19
5.5	5.100	20.43	394	1.85	443	0.83	200	1.192	0.02

is an inert substance; it does not participate in chemical reactions [6]. The mix proportion is listed in Table 2.

The water-to-cement ratio was kept constant at 0.5. Upon adding basalt fibers, the workability was excessively decreased. Therefore, Sika Viscocrete-180G has a specific gravity of 1.065 gm/cm^3 and was used as a high-range water reducer and super plasticizing admixture having a polycarboxylates polymer base.

The prepared mixture was cast into the column mold and compacted with a 16 mm steel rounded end rod to ensure that the concrete reached all parts inside the mold, as shown in Figure 4. Three or more cylinders with (100x200) mm size were also cast from the same mixture as control specimens for testing cylinder compressive strength. All specimens were entirely covered with polyethylene sheets to prevent water evaporation. Twenty-four hours after casting, the specimens were de-molded, then cured in water for 28 days. One day before testing, the specimens were taken out of the water and left to dry to examine in a saturated, dry surface condition.

Figure 3. Chopped basalt fibers

TABLE 2. Mix proportions of concrete used in the experiments

Mix symbol	Cement content, kg/m^3	Fine aggregate, kg/m^3	Coarse aggregate, kg/m^3	Water content, kg/m^3	Basalt fibers		HRWRA	
					Vf * %	Content, kg/m^3	% **	Dosage, L/m^3
MBF0.00	430	823	847	215	0.00	0.00	0.00	0.00
MBF0.30	430	823	847	215	0.30	8.43	0.75	3.23
MBF0.60	430	823	847	215	0.60	16.90	1.25	5.38

*** Volume fraction of concrete**
**** Percent of cement content**

A data logger was used to record the loads and displacements at each increment.

For (100x200) mm concrete cylinder specimens, a Matest compressive testing device with 2500 kN capacity was used. All columns and control specimens were tested at 28-day ages.

2. 3. Test Setup and Instrumentation A compression bearing was subjected to the top section of the column. Two steel bolsters representing bases support the column from top and bottom. They were made of a steel ring have a diameter slightly larger than the column diameter. These bolsters were used to install the column in the testing device, as shown in Figure 5. Rubber pads of 150 mm diameter and 5 mm thickness were placed between the base of the bolsters and the concrete column at the top and bottom to avoid the impact load. A universal testing machine of 1000 kN capacity was applied to test the columns. A load cell of 1000 kN capacity was placed over the upper bolster to record the load increment. An LVDT tool was used between the upper and lower bolsters to record the axial displacement.

Figure 4. Concrete pouring into a mold

Figure 5. Test setup and instrumentation

3. EXPERIMENTAL RESULTS AND DISCUSSION

The devices used to record the loads and displacements were tested before the actual loading of column specimens. The column was preloaded by 40 kN for 3 minutes to observe the measuring system. Next, the actual loading was carried out with an increase of 40 kN per grade up to 160 kN, then 20 kN until failure. Each load grade was sustained for 2 minutes to observe the appearance of cracks and allow the stability of the load to record the data. The loading system is shown in Figure 5.

3. 1. Compressive Strength Results Three or more concrete cylinders were tested per every mix at 28 days, and the average value was regarded for compressive strength. Test results are shown in Table 3.

According to the compressive strength results, it is clear that raising basalt fiber content to 0.6 % enhances compressive strength. However, 0.3 % of basalt fibers increase compressive strength more than 0.6 %. The best increase in compressive strength was 23.69% at 0.3% basalt fibers. Comparing this result to Kirthika and Singh's [9] results, they found that 0.5% increased compressive strength by 26.8%. Also, Dilbas and Cakir [15] found that 0.25% of basalt fibers (BF) awarded the best compressive strength.

The micro diameter of basalt fibers awards plenty of filaments. The low percentage of basalt fiber can orient in all directions within the concrete matrix. The bonding strength between the filament and concrete matrix increases because of its micro diameter, giving high internal confinement and reducing early shrinkage. These features enhance compressive strength.

On the other hand, the microfilament is flexible and can be bent and curled during mixing and running in a concrete mixture. When the number of filaments is extra-large, the percentage of curled ones increases to entrap dry mortar inside and form voids. Therefore, the number of voids increases inside the concrete microstructure, and the voids increment reduces the strength. Furthermore, the micro diameter of filaments raises the fibers' surface area to increase the water molecules' demand. So not all filaments will get the quantity of water they need to adhere to them. When the fiber content is relatively high, the number of non-bonded filaments increases, besides increasing the voids formed by the curled fibers; therefore, the strength comparatively decreases.

TABLE 3. Cylinder compressive strength per basalt fiber content

BF content, %	Comp. strength, f'c, MPa	Percentage of increase in f'c, %	SD	COV
0.00	32.42	0.00	1.516	0.047
0.30	40.10	23.69	1.091	0.027
0.60	35.46	9.38	1.346	0.038

3. 2. Short Column Results Table 4 lists the test results of cracking and ultimate loads sustained by short columns with the corresponding longitudinal displacements. The columns are divided into three groups according to the basalt fiber content. Each group consists of three columns with three different tie spacing. Columns are coded with the letter "C" to indicate a circular column, the letter "S" indicates tie spacing, and the number following it refers to tie spacing value. The other number refers to the basalt fiber percentage. For instance, CS80-0.3 represents a short circular column with 80 mm tie spacing and 0.3 % of basalt fibers.

Short columns without fibers sustain more than 50 % of the failure load before cracking, whereas incorporating basalt fibers into the concrete matrix raised the cracking load to about three-quarters of the failure load.

3. 3. Effect of Basalt Fiber Content on Short Column Loading Capacity The addition of basalt fibers to the concrete matrix enhanced short column capacity. The 0.3 % of basalt fibers increased loading capacity by more than 50 % at the cracking state and between (15-19) % at the ultimate state. At 0.6 % of basalt fiber content, the cracking load was increased by about 50 % over the no-fiber short columns, while at the maximum loading, the increase was between (7.7-11.0) %. Generally, 0.3 % of basalt fiber enhanced the bearing capacity of the short column more than that of 0.6 % at cracking and ultimate state, as shown in Figures 6 and 7. The results also clarified that the effect of basalt fibers on cracking loads was more than on the maximum loads. The cracking load was about 55% of the ultimate load for no fiber columns, while this ratio increased to 75% approximately for BFRC columns, as shown in Figure 8.

On the other hand, basalt fibers reduced the longitudinal displacement at the cracking state. However, at the ultimate state, there was no evident effect for the fibers on the longitudinal shortening.

TABLE 4. Short-column test results for cracking and ultimate state

Column ID	BF content	f'c	Cracking load, Pcr, kN	Δcr, mm	Ultimate load, Pu, kN	Ultimate displacement, Δu, mm	Pcr/Pu	Pcr/Pcro
CS 80-0.00	0	32.42	256.40	1.65	470.18	3.2	0.545	1.00
CS120-0.00	0	32.42	258.89	1.86	461.64	3.0	0.561	1.00
CS180-0.00	0	32.42	257.05	1.80	453.72	3.2	0.567	1.00
CS 80-0.30	0.3	40.10	405.80	1.20	558.65	3.2	0.726	1.58
CS120-0.30	0.3	40.10	406.87	1.22	532.73	3.6	0.764	1.57
CS180-0.30	0.3	40.10	399.65	1.18	521.33	3.7	0.767	1.55
CS 80-0.60	0.6	35.46	386.50	1.28	521.67	3.7	0.741	1.51
CS120-0.60	0.6	35.46	386.02	1.34	498.73	3.7	0.774	1.49
CS180-0.60	0.6	35.46	382.50	1.33	488.50	3.2	0.783	1.49

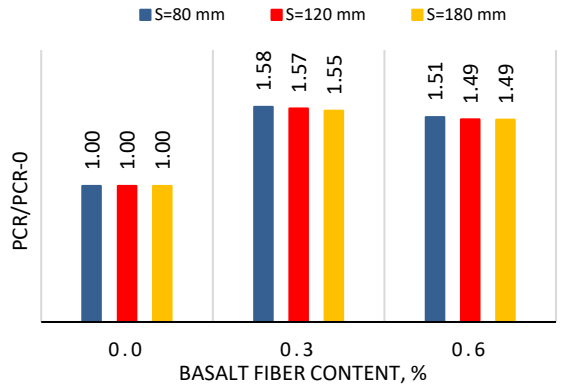

Figure 6. Cracking load increment ratio vs. basalt fiber content

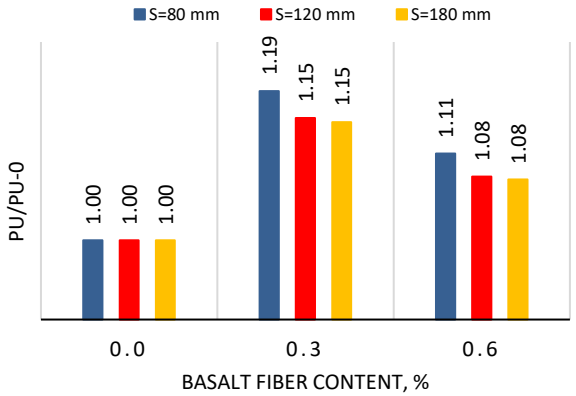

Figure 7. Ultimate load increment ratio vs. basalt fiber content

As stated previously, basalt microfilaments with 16-18 μm diameter can bond firmly with concrete matrix to form a spatial network surrounding the granules of coarse aggregate. Therefore, that network can improve the combination of concrete ingredients. The spatial network encases the coarse aggregate to hinder its movement during compression. Also, it can enhance the interfacial transition zone between coarse aggregate and cement paste and reduce the number and size of voids inside the concrete microstructure. These improvements are positively reflected in the concrete strength and are more effective when filament distribution is uniform and in all orientations. When the number of filaments steadily increases, and some remain uncombined to the matrix, the voids increase and cause reduced strength comparatively.

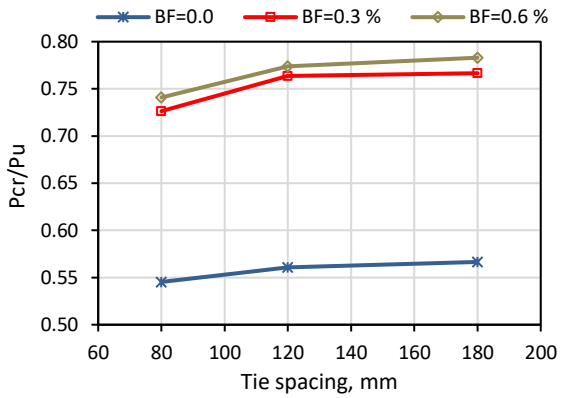

Figure 8. Effect of basalt fibers on cracking and ultimate loads

High bonding strength due to the micro diameter with the huge number of combined filaments requires more energy to overcome the bonding strength between filaments and concrete matrix. These features enhance cracking loading. Therefore, the cracking loads in BFRC short columns are more than in no fiber columns. Similar reasons apply to the longitudinal displacement of BFRC short columns.

3. 4. Effect of Tie Spacing On Loading Capacity

Three tie spacing were used in the three groups of columns: 80 mm, 120 mm, and 180 mm, to clarify the influence of changing tie spacing along with basalt fiber

content on the cracking and ultimate loading capacity. According to the results, the smaller the tie spacing, the slightly higher the loading capacity of the short column at the peak state.

For conventional concrete columns, the increment ratio in ultimate load was 1.85 % and 3.63 %. For BFRC columns with 0.3 %, the increment ratio was 4.9 % and 7.2 % upon reducing spacing by 40 mm and 100 mm, respectively. For 0.6 % of basalt fibers, the increment ratio in ultimate load was 4.6 % and 6.8 %, respectively, as shown in Figure 9. The increase in the loading capacity of BFRC columns was more than that of conventional concrete columns.

At a cracking state, non-apparent variation in the loads occurred for the same basalt fiber content, which is considered logical since the effect of fibers and steel ties occurs after cracking, as illustrated in Table 4.

Both ties and basalt filaments provide confinement to the concrete. Steel ties externally confine the concrete core, and basalt filaments provide internal confinement to the matrix because of their relatively high bond strength with concrete. The external and internal confinements restrict the concrete from expanding laterally. Therefore, they enhance the concrete strength in tension and compression. Additionally, the internal confinement of basalt fiber can improve the compressive strength and delay the initial cracking, which, in turn, increases the loading capacity of short columns.

However, the influence of internal confinement caused by basalt fiber on small specimens of concrete cylinders is more pronounced than on larger column specimens. That may be because the small size of concrete cylinders awards further restriction of stress transmission through small size.

3. 5. Failure Pattern Through the test, columns did not originate transverse cracks, while vertical cracks occurred near supports before failure. Upon increasing the load, the cracks developed gradually, then the concrete was crushed, and the column failed. However, the steel ties remained sound when the columns were damaged. All the columns have failed due to the crushing of concrete at the upper or lower third or both ends near the bolsters, as illustrated in Figure 10. That was because the stresses were concentrated near the loading point. During crack propagation and before failure, the concrete cover fell off. At fracture, the cracks propagated longitudinally and focused near the bolsters. After the peak, the load dropped slowly but never less than 40 % of the column loading capacity, which refers to ductility acquired by the column when adding basalt fibers. Generally, BFRC short columns were cracked later than the non-fibrous columns.

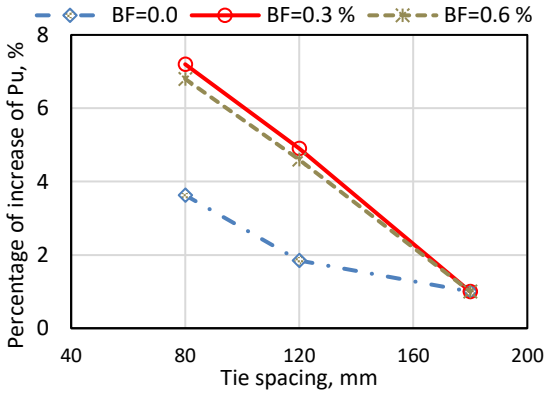

Figure 9. Influence of basalt fibers and tie spacing on ultimate load

4. NUMERICAL ANALYSIS OF COLUMNS

A numerical analysis via Abaqus software was developed to trace the structural behavior of columns under axial compressive loading. It was performed by displacement control to capture the load at each increment.

4. 1. Numerical Simulation of Columns The analyzed column consists of a concrete column with a circular section of 150 mm diameter, longitudinal rebars of 8 mm diameter, transverse ties of 5.1 mm diameter, and steel supporting plates. The concrete column and steel plates are discretized with a 3-dimensional continuum of 8 nodes and a reduced integration element (C3D8R). Steel rebars are discretized by 2 nodded link elements (T3D2). C3D8R has 8 nodes with 3 degrees of freedom per node. This element can model solids in 3 dimensions with or without reinforcement. It can consider tensile cracking, compressive crushing, and large strains [33]. T3D2 element is used to model one-dimensional rebar regarding axial strain only as a truss element[1]. Figure 11 depicts the discretization of the columns.

Figure 10. Failure patterns of short columns

[1] http://www.wiley.com/go/permissions

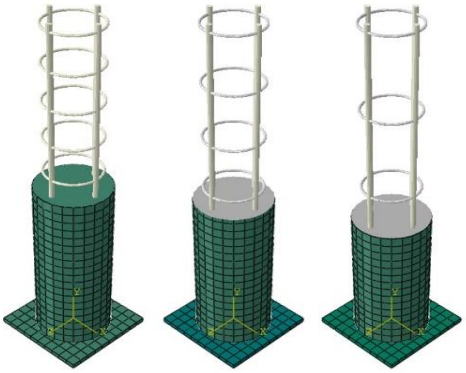

Figure 11. The meshing of concrete columns and rebars

The relationship between the concrete and rebars is assigned via the embedded region. The rebars are embedded inside the host region of concrete. The steel plates are constrained as a rigid body to prohibit deformation during loading. The lower plate is assigned as fixed support by preventing the transition and rotation in all directions. The load is applied to the upper steel plate. The elements of all parts are seeded by a 20 mm mesh size in all orientations. The interaction between the steel plates and concrete column is selected to be a contact with the normal behavior of hard contact type to prevent penetration between them and tangential behavior with a friction coefficient of 0.45 between concrete and steel. The analysis is done with a static general step.

4. 2. Material Models The elastic behavior of concrete is defined by its modulus of elasticity and Poisson's ratio. The plastic behavior of concrete is defined by the concrete damage plasticity (CDP) model to define different transition laws of strength under compression and tension [33]. To define the CDP model, the stress-inelastic strain including compression hardening and softening, and tensile stiffening are determined according to the experimental results for compressive strength. Hognestad and Eurocode, Eu-2004 [24] formula is adopted to capture the compressive stresses at the successive strains as follows;

$$\sigma_c = f_c' \left[2\left(\frac{\varepsilon_o}{\varepsilon_{co}} - \left(\frac{\varepsilon_o}{\varepsilon_{co}}\right)^2\right)\right] \quad (1)$$

$$\varepsilon_o = \frac{0.4\, f_c'}{E_c} \quad (2)$$

$$E_c = 3320\sqrt{f_c'} + 6900 \quad (3)$$

$$\varepsilon_{co} = \frac{2f_c'}{E_c} \quad (4)$$

$$\varepsilon_{pl.} = \varepsilon - \frac{\sigma_c}{E} \quad (5)$$

$$d_c = 1 - \frac{\sigma_c}{f_rc} \quad (6)$$

where:
σ_c = Compressive stress at corresponding strain, MPa
ε_{co} = Compressive strain at compressive strength.
ε_o = Strain at 40% of compressive strength (elastic limit).
E_c = Modulus of elasticity, MPa.
$\varepsilon_{pl.}$ = Plastic strain, and dc = damage parameter

The yield tensile strength is considered (1/10 -1/12) of compressive strength. Steel rebars are defined by the yield stresses for 5.1 mm bars and 8 mm bars, as determined experimentally. The failure surface of the finite elements is defined by the five parameters adopted in Abaqus, which are the dilation angle (ψ), eccentricity (Ɛ), the ratio of biaxial to uniaxial stress (fbo/fco), the shape of failure surface (K), and the viscosity parameter (μ). These values are illustrated in Table 5.

4. 3. Model Validation and Analysis Results The performed finite element model was validated by comparing its results with the experimental ones. The ultimate loads, longitudinal displacements, and crack patterns are compared with the experimental results to gauge the efficiency of the simulated model for predicting the structural behavior of columns.

4. 4. Loads and Longitudinal Displacements The finite element (FE) loads and longitudinal displacements (Δ) are illustrated in Table 6. At the cracking state, the FE loads underestimate the experimental ones because the FE results in Abaqus depend on the cracking stress of concrete, which is determined to be 40 % of compressive strength. The ratio between an experiment to FE cracking loads ranges between (1.08-1.09) for columns without fibers and between (1.21-1.23) for BFRC columns. The increase in cracking loads for no fiber columns by (8-9) % indicates that cracking does not occur at 40 % of concrete strength. That is due to the effect of ties in the columns. The additional change in fibers column experimental results refer to the influence of basalt fiber, where the microfilaments provide confinement to the concrete matrix. That confinement delays cracking and restricts crack initiation and propagation until it acquires enough energy to overcome the bonding forces between microfilaments and the matrix. For columns without fiber, the cracking displacements underestimate the experimental results. For columns with fibers, the FE cracking loads underestimate the experimental ones by (8-9) %. That reflects the action of basalt fibers in restricting the cracking and providing confinement.

At peak state, the FE loads approach the experimental ones. The ratio between an experiment to FE loads ranges between (0.94-1.03). The FE displacements are also close to the experimental results. The ratio between the experiment to FE displacement is (0.91-1.10). The results also clarify that the displacement increases with increasing tie spacing for all basalt fiber content, which is due to the increase of confinement effect of ties.

Generally, the displacement increases more than conventional concrete upon adding basalt fibers. Figures 12, 13, and 14 depict relationships between loads and longitudinal displacement for whole columns. According to these figures, the columns' behavior is similar until cracking loads, after which differences appear up to failure. After maximum loads, the columns continue in almost horizontal loads with increasing longitudinal displacement indicating the ductility of the columns.

4. 5. Crack Pattern The numerical analysis results showed that all columns failed due to concrete crushing. The loading in Abaqus was carried out by displacement control. Upon increasing loads, the cracks initiated near the upper and lower supports then propagated to the third bottom in some columns or to the mid-length in others, as illustrated in Figure 15. However, the failure pattern of the FEA corresponded to the experimental results.

TABLE 5. The properties of materials used to simulate the short columns in Abaqus

Material	Properties					
Concrete	Elastic modulus, Ec				Poisson's ratio	
	Variable, according to f'c				0.18	
	ψ	ε	f_{bo}/f_{co}	K	μ	
	25	0.1	1.16	0.67	1E-12	
Steel rebars	Diameter = 8 mm			Diameter = 5.1 mm		
	Es	Yield stress	Poisson's ratio	Es	Yield stress	Poisson's ratio
	200 GPa	563 MPa	0.30	200 GPa	394 MPa	0.30

TABLE 6. The FEA results compared to experimental results

Column ID	Pcr, kN		Pcr	Δcr, mm		Δcr	Pu, kN		Pu	Δu, mm		Δu
	EXP	FEA	EXP/FEA	EXP	FEA	EXP/FEA	EXP	FEA	EXP/FEA	EXP	FEA	EXP/FEA
CS 80-0.00	256.4	237.8	1.08	1.65	0.97	1.71	470.18	495.64	0.95	3.2	3.17	1.01
CS120-0.00	258.9	238.2	1.09	1.86	0.97	1.91	461.64	489.39	0.94	3.0	3.24	0.93
CS180-0.00	257.1	237.6	1.08	1.80	0.97	1.86	453.72	482.34	0.94	3.2	3.57	0.90
CS 80-0.30	405.8	331.9	1.22	1.20	1.46	0.82	558.65	539.99	1.03	3.2	3.49	0.92
CS120-0.30	406.9	330.6	1.23	1.22	1.46	0.84	532.73	533.39	1.00	3.6	3.69	0.98
CS180-0.30	399.7	329.2	1.21	1.18	1.46	0.81	521.33	526.04	0.99	3.7	3.94	0.94
CS 80-0.60	386.5	320.2	1.21	1.28	1.46	0.88	521.67	510.83	1.02	3.7	3.37	1.10
CS120-0.60	386.0	318.9	1.21	1.34	1.46	0.92	498.73	504.37	0.99	3.7	3.46	1.07
CS180-0.60	382.5	317.3	1.21	1.33	1.46	0.91	488.50	497.25	0.98	3.2	3.51	0.91

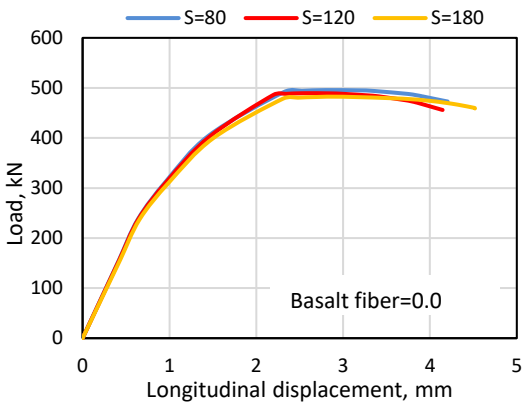

Figure 12. Load-longitudinal displacement relation of the column without basalt fiber

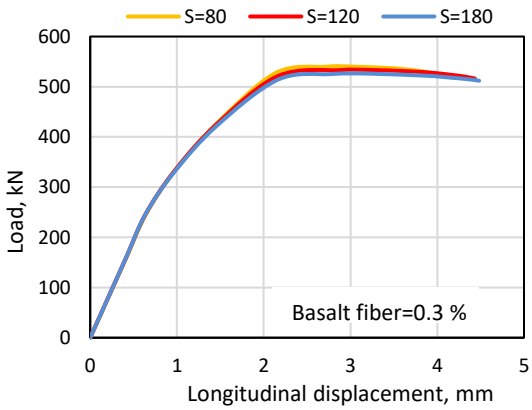

Figure 13. Load-longitudinal displacement relation of the column with 0.3% basalt fiber

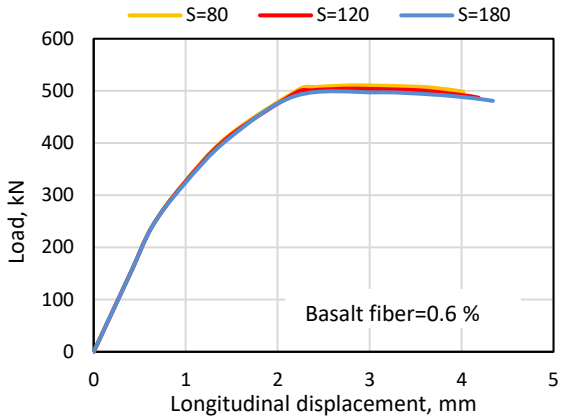

Figure 14. Load-longitudinal displacement relationship of the column with 0.6% basalt fiber

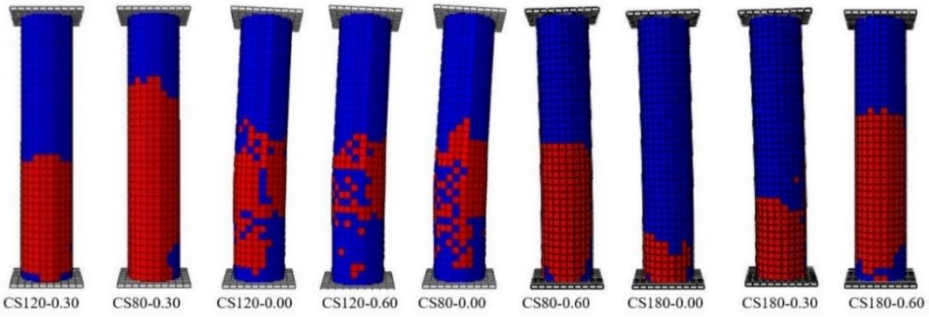

Figure 15. A crack pattern of the columns

The longitudinal bars and transverse ties did not reach yielding at the ultimate loads for all columns. That referred to the failure was occurred due to concrete crushing. The longitudinal bars sustained (70-88) % of yield stress at the maximum loads. The longitudinal bars of columns CS80-0.3, CS120-0.3, and CS180-0.3 endure the highest stress. On the other hand, the middle tie bore the higher stress at the ultimate load, which indicated a column tendency to buckle.

4. 6. Parametric Study A numerical study was performed to demonstrate the effect of reinforcement ratio on the column loading capacity by changing the longitudinal bar diameter. Three bar diameters were adopted: 6mm, 8mm, and 10mm, to award 0.64 %, 1.13 %, and 1.78 % reinforcement ratios (ρ), respectively. The yield stress of the bar was not changed, and all other parameters remained the same. The results of FEA are illustrated in Table 7.

TABLE 7. Loading capacity and Longitudinal displacement upon changing reinforcement ratio

Column ID	db=6 mm, ρ=0.64 %		db=8 mm, ρ=1.13 %		db=10 mm, ρ=1.78 %	
	Pu, kN	Δu, mm	Pu, kN	Δu, mm	Pu, kN	Δu, mm
CS 80-0.00	458.54	3.24	495.64	3.17	510.57	1.95
CS120-0.00	451.36	3.47	489.39	3.24	500.00	1.99
CS180-0.00	444.83	3.58	482.34	3.57	495.24	2.10
CS 80-0.30	504.71	3.49	539.99	3.49	575.30	2.30
CS120-0.30	496.10	3.68	533.39	3.69	564.60	2.34
CS180-0.30	489.20	3.94	526.04	3.94	554.75	2.36
CS 80-0.60	473.98	3.44	510.83	3.37	530.96	2.08
CS120-0.60	465.73	3.49	504.37	3.46	521.03	2.10
CS180-0.60	460.90	3.53	497.25	3.51	514.00	2.20

According to the results of numerical analysis, increasing the reinforcement ratio raises the loading capacity of the column for all basalt fiber contents. The 0.3 % basalt fiber content causes the highest increment in column loading capacity.

At 0.0 % basalt fiber ratio, raising the reinforcement ratio from 0.64 % to 1.13 % and 1.78 % increases the maximum loading by 8 % and 11 %, respectively. While at 0.3 % and 0.6 % basalt fiber content, increasing the reinforcement ratio from 0.64 % to 1.13 % and 1.78 % raises the ultimate loading of the column by (7.5-8) % and (12-14) %, respectively.

On the other hand, for the same tie-spacing, increasing the reinforcement ratio raises the load capacity of columns where the 0.3 % basalt fiber content awarded the highest increment in all cases, as shown in Figures 16, 17, and 18.

Despite increasing reinforcement ratio in the column, the failure remained due to concrete crushing before the rebars reached yielding.

When the tie-spacing decreases and the reinforcement ratio increases, the loading capacity of the column further increases. It is well known that the stresses in columns are borne by concrete and steel rebar. Therefore, increasing the area of rebars with its relatively high yield stress increases the stresses sustained by the column section. Also, decreasing tie spacing increases external confinement on a concrete core to raise the loading capacity of the column.

The longitudinal displacement slightly increased upon increasing tie spacing. However, it decreased with increasing the reinforcement ratio. Furthermore, for a 1.78 % reinforcement ratio, the lowest longitudinal displacement was recorded numerically. Also, no significant changes occurred in longitudinal displacement at a higher reinforcement ratio.

Axial deformation is proportional to the axial load and column length and inversely proportional to the sectional area and elastic modulus. Since column length, cross-sectional area, and elastic modulus are constant, the change in rebar area is considered the prime determinant for axial deformation besides the load. Therefore, when the reinforcement area increases, the longitudinal displacement decreases.

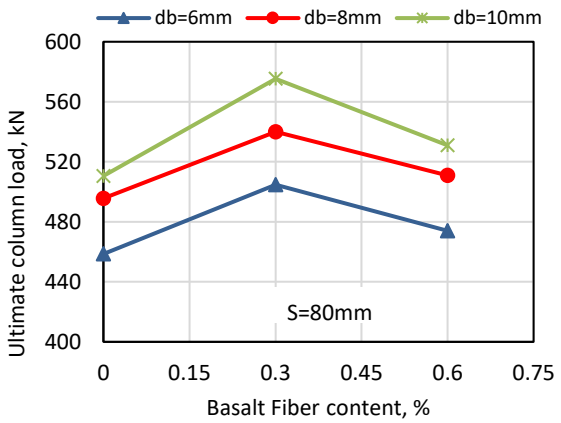

Figure 16. The effect of bar diameter on loading capacity when tie spacing is 80 mm

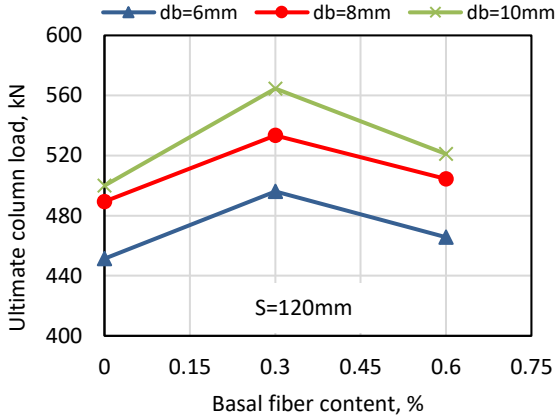

Figure 17. The effect of bar diameter on loading capacity when tie spacing is 120 mm

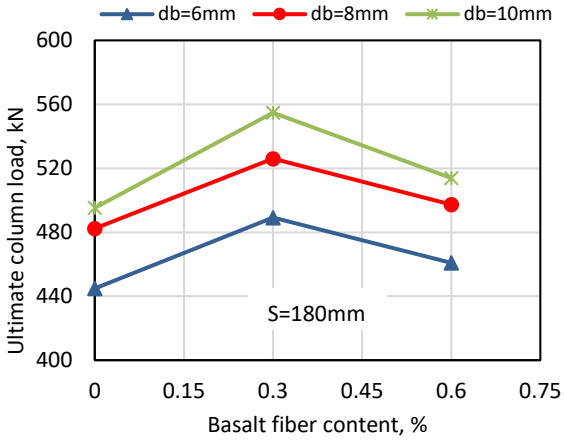

Figure 18. The effect of bar diameter on loading capacity when tie spacing is 180 mm

5. CONCLUSIONS

This research presents experimental and numerical investigations on the combined effect of basalt fibers and tie spacing on the behavior of short columns. Loading capacity at cracking and ultimate state with corresponding longitudinal displacements and the crack pattern is experimentally discovered. Then a numerical analysis is performed via Abaqus software to clarify the effect of reinforcement ratio on the loads and displacements. The following conclusion can derive:

Short concrete columns without fibers sustained more than 50 % of the failure load before cracking. Addition of basalt fiber delays cracking and increases the cracking load to about 75 % of the failure load. 0.3 % of basalt fibers increases the compressive strength and short column's load at cracking and ultimate state more than 0.6 %. The impact of basalt fibers on cracking load is more pronounced than on maximum load.

Basalt fiber reduces the longitudinal displacement at the cracking state. However, it has no evident effect on the displacement at the ultimate state.

The smaller the tie spacing, the slightly higher the ultimate load of the short column. Adding basalt fibers reduces the longitudinal displacement at cracking. The longitudinal displacement increases upon increasing tie spacing.

The numerical analysis awarded results close to the experimental ones at ultimate loading. Also, the empirical and numerical failure was the same for all columns by crushing concrete, while the longitudinal and tie rebars did not yield at maximum load.

Increasing the reinforcement ratio with keeping tie-spacing constant increases the loading capacity of columns. The increment in ultimate loads increases with decreasing tie spacing.

6. REFERENCES

1. Rajasekaran, A., Raghunath, P. and Suguna, K., "Effect of confinement on the axial performance of fibre reinforced polymer wrapped rc column", ***American Journal of Engineering and Applied Sciences***, Vol. 1, No. 2, (2008), 110-117.
2. Al-Kharabsheh, B.N., Arbili, M.M., Majdi, A., Alogla, S.M., Hakamy, A., Ahmad, J. and Deifalla, A.F., "Basalt fibers reinforced concrete: Strength and failure modes", ***Materials***, Vol. 15, No. 20, (2022), 7350. https://doi.org/10.3390/ma15207350
3. Aljazaeri, Z. and Al-Jaberi, Z., "Numerical study on flexural behavior of concrete beams strengthened with fiber reinforced cementitious matrix considering different concrete compressive strength and steel reinforcement ratio", ***International Journal of Engineering, Transactions A: Basics***, Vol. 34, No. 4, (2021), 793-802. https://doi.org/10.5829/ije.2021.34.04a.05
4. Solhmirzaei, R. and Kodur, V., "Modeling the response of ultra high performance fiber reinforced concrete beams", ***Procedia Engineering***, Vol. 210, (2017), 211-219. https://doi.org/10.1016/j.proeng.2017.11.068
5. Systèmes, D., *Getting started with abaqus: Interactive edition*. 2014, Version.
6. Ayub, T., Shafiq, N. and Nuruddin, M.F., "Mechanical properties of high-performance concrete reinforced with basalt fibers", ***Procedia Engineering***, Vol. 77, (2014), 131-139. https://doi.org/10.1016/j.proeng.2014.07.029
7. Committee, A., "Building code requirements for structural concrete (aci 318-08) and commentary, American Concrete Institute. (2008).
8. Qin, J., Qian, J., Li, Z., You, C., Dai, X., Yue, Y. and Fan, Y., "Mechanical properties of basalt fiber reinforced magnesium phosphate cement composites", ***Construction and Building Materials***, Vol. 188, (2018), 946-955. https://doi.org/10.1016/j.conbuildmat.2018.08.044
9. Kirthika, S. and Singh, S., "Experimental investigations on basalt fibre-reinforced concrete", ***Journal of The Institution of Engineers (India): Series A***, Vol. 99, (2018), 661-670. https://doi.org/10.1007/s40030-018-0325-4
10. Ramesh, B. and Eswari, S., "Mechanical behaviour of basalt fibre reinforced concrete: An experimental study", ***Materials Today: Proceedings***, Vol. 43, (2021), 2317-2322. https://doi.org/10.1016/j.matpr.2021.01.071
11. Jia, M., Xie, W., Yu, K. and Qian, K., "A comparative study of the mechanical properties of basalt fiber and basalt grille reinforced concrete composites and theoretical prediction", ***Journal of Natural Fibers***, Vol. 19, No. 13, (2022), 5862-5879. https://doi.org/10.1080/15440478.2021.1902451
12. Sun, X., Gao, Z., Cao, P. and Zhou, C., "Mechanical properties tests and multiscale numerical simulations for basalt fiber reinforced concrete", ***Construction and Building Materials***, Vol. 202, (2019), 58-72. https://doi.org/10.1016/j.conbuildmat.2019.01.018
13. Li, Z.-X., Li, C.-H., Shi, Y.-D. and Zhou, X.-J., "Experimental investigation on mechanical properties of hybrid fibre reinforced concrete", ***Construction and Building Materials***, Vol. 157, No., (2017), 930-942. https://doi.org/10.1002/suco.201500216
14. Dilbas, H. and Çakır, Ö., "Influence of basalt fiber on physical and mechanical properties of treated recycled aggregate concrete", ***Construction and Building Materials***, Vol. 254, (2020), 119216. https://doi.org/10.1016/j.conbuildmat.2020.119216
15. Ghasem Ghanbari, P., Momeni, M., Mousivand, M. and Bayat, M., "Unconfined compressive strength characteristics of treated peat soil with cement and basalt fibre", ***International Journal of Engineering, Transactions B: Applications***, Vol. 35, No. 5, (2022), 1089-1095. https://doi.org/10.5829/ije.2022.35.05b.24
16. High, C., Seliem, H.M., El-Safty, A. and Rizkalla, S.H., "Use of basalt fibers for concrete structures", ***Construction and Building Materials***, Vol. 96, (2015), 37-46. https://doi.org/10.1016/j.conbuildmat.2015.07.138
17. Krassowska, J. and Kosior-Kazberuk, M., "Failure mode of basalt fibre reinforced concrete beams", in IOP Conference Series: Materials Science and Engineering, IOP Publishing. Vol. 471, (2019), 052043.
18. Hirde, S. and Shelar, S., "Effect of basalt fiber on strength of cement concrete", ***International Journal of Current Engineering and Technology***, Vol. 7, No. 2, (2017), 600-602.
19. Iyer, P., Kenno, S.Y. and Das, S., "Mechanical properties of fiber-reinforced concrete made with basalt filament fibers", ***Journal of Materials in Civil Engineering***, Vol. 27, No. 11, (2015), 04015015. https://doi.org/10.1061/(asce)mt.1943-5533.0001272
20. Hoshitha, T.S.S., Rao, T.C. and Rao, T.G., "Effect of lateral confinement on short columns under uni-axial compression", in AIP Conference Proceedings, AIP Publishing LLC. Vol. 2297, (2020), 020015.
21. Jabbar, A.M., Hamood, M.J. and Mohammed, D.H., "Mitigation of the factors affecting the autogenous shrinkage of ultra-high performance concrete", ***Engineering and Technology Journal***,

Vol. 39, No. 12, (2021), 1860-1868. https://doi.org/10.30684/etj.v39i12.2155

22. Jabbar, A.M., Hamood, M.J. and Mohammed, D.H., "The effect of using basalt fibers compared to steel fibers on the shear behavior of ultra-high performance concrete t-beam", ***Case Studies in Construction Materials***, Vol. 15, (2021), e00702. https://doi.org/10.1016/j.cscm.2021.e00702
23. Jabbar, A.M., Mohammed, D.H. and Hamood, M.J., "Using fibers instead of stirrups for shear in ultra-high performance concrete t-beams", ***Australian Journal of Structural Engineering***, Vol. 24, No. 1, (2023), 36-49. https://doi.org/10.1080/13287982.2022.2088654
24. En, B., "1-1. Eurocode 2: Design of concrete structures–part 1-1: General rules and rules for buildings", ***European Committee for Standardization (CEN)***, (2004). https://doi.org/ICS13.220.50;91.010.30;91.080.40
25. Jamshaid, H., "Basalt fiber and its applications", ***Journal of Textile Engineering & Fashion Technology***, Vol. 1, No. 6, (2017), 254-255. https://doi.org/10.15406/jteft.2017.01.00041
26. John, V.J. and Dharmar, B., "Influence of basalt fibers on the mechanical behavior of concrete—a review", ***Structural Concrete***, Vol. 22, No. 1, (2021), 491-502. https://doi.org/10.1002/suco.201900086
27. Mokhtar, S.F. and Lim, N.H.A.S., "Effects of ties distributions on short column strength siti fatimah mokhtar, dr. Nor hasanah abdul shukor lim".
28. Naji, A., Al-Jelawy, H., Hassoon, A. and Al-Rumaithi, A., "Axial behavior of concrete filled-steel tube columns reinforced with steel fibers", ***International Journal of Engineering, Transactions C: Aspects***, Vol. 35, No. 9, (2022), 1682-1689. https://doi.org/10.5829/ije.2022.35.09c.02
29. Nemati Aghamaleki, S., Naghipour, M., Vaseghi Amiri, J. and Nematzadeh, M., "Experimental study on compressive behavior of concrete-filled double-skin circular tubes with active confinement", ***International Journal of Engineering, Transactions A: Basics***, Vol. 35, No. 4, (2022), 819-829. https://doi.org/10.5829/ije.2022.35.04a.22
30. International, A., "Astm c150/c150m-15, standard specification for portland cement, american standard for testing and materials, ASTM West Conshohocken, PA, USA. (2015).
31. EN, C., *10002-5, metallic materials–tensile testing–part 5: Method of testing at elevated temperature*. 1992, Brussels.
32. No, I.S., "For aggregates of natural resources used for concrete and construction", Baghdad, Iraq, (1984).
33. Fiore, V., Scalici, T., Di Bella, G. and Valenza, A., "A review on basalt fibre and its composites", ***Composites Part B: Engineering***, Vol. 74, (2015), 74-94. https://doi.org/10.1016/j.compositesb.2014.12.034

Persian Abstract

چکیده

این مقاله اثر افزودن الیاف بازالت به یک زمینه بتنی و تغییر فاصله اتصال را بر رفتار ستون‌های بتنی کوتاه نشان می‌دهد، زیرا ستون‌های کوتاه قوی‌تر از ستون‌های بلند هستند و عمدتاً در سازه‌ها استفاده می‌شوند. همچنین تأثیر تغییر نسبت آرماتور بر رفتار ستون به صورت عددی کشف شده است. سه بخش حجمی از الیاف بازالت و فاصله سه کراواتی اتخاذ شده است. نتایج نشان می دهد که ستون های بدون الیاف بیش از ۵۰ درصد بار شکست را قبل از ترک خوردگی تحمل می کنند، در حالی که این درصد با افزودن الیاف بازالت به بتن به ۷۵ درصد افزایش می یابد. ۰.۳٪ الیاف بازالت استحکام فشاری، ترک خوردگی و بارهای ستون نهایی را بهتر از ۰.٦٪ افزایش می دهد. به همین ترتیب، تاثیر الیاف بازالت بر بار ترک بیشتر از حداکثر بار ستون است. ستون های فیبر بازالتی در حالت ترک، جابجایی طولی کمتری نسبت به ستون های بدون الیاف نشان می دهند. کوتاه شدن با افزایش فاصله کراوات افزایش می یابد، در حالی که کاهش فاصله کراوات به سختی بار نهایی ستون را افزایش می دهد. تجزیه و تحلیل عددی نتایج نزدیک به نتایج تجربی را ارائه می دهد و نشان می دهد که افزایش نسبت آرماتور ظرفیت بار ستون را افزایش می دهد. برای همان فاصله اتصال، افزایش نسبت آرماتور ظرفیت بارگذاری ستون ها را افزایش می دهد و جابجایی طولی به سختی با افزایش فاصله افزایش می یابد. به طور کلی، الیاف بازالت، ترک خوردگی را به تاخیر می اندازد و ظرفیت بارگذاری ستون را بهبود می بخشد.